PHYSICAL REVIEW B VOLUME 18, NUMBER 8 15 OCTOBER 1978

Quantum oscillations and the Fermi surface of $2H$-TaS_2

S. J. Hillenius and R. V. Coleman
Department of Physics, University of Virginia, Charlottesville, Virginia 22901
(Received 9 May 1978)

Quantum oscillations in the magnetoresistance and susceptibility of $2H$-TaS_2 have been used to determine Fermi-surface cross sections. Eleven frequencies in the range from 0.04 to 6.44 MG have been observed corresponding to sections arising from the charge-density-wave transition at 75 K. Comparison to the frequencies observed in $4Hb$-TaS_2 shows that the Fermi-surface cross sections are similar in both the $2H$ and $4Hb$ phases indicating relatively little charge transfer between octahedral and trigonal prismatic layers in $4Hb$-TaS_2. The angular dependence observed for a number of sections in $2H$-TaS_2 shows a $\sec\theta$ dependence characteristic of cylinders while others show a more three-dimensional behavior in contrast to $4Hb$-TaS_2 where all of the lowest frequencies show a $\sec\theta$ dependence. Comparison to results on $2H$-$TaSe_2$ and to band-structure calculations and band-folding models will also be made.

I. INTRODUCTION

The layer-structure dichalcogenides TaS_2 and $TaSe_2$ show a variety of charge-density-wave (CDW) transitions that have been detected in transport[1-6] measurements and in x-ray,[7] electron,[1,4] and neutron-diffraction[8-10] experiments. All of the well-studied phases, including $2H$ (trigonal prismatic coordination), $1T$ (octahedral coordination), and $4Hb$ (mixed coordination), show one or more CDW transitions in a temperature range from 20 to 500 K. A number of band-structure calculations[11-13] have been made for the high-temperature non-CDW phases of these materials, and several recent model calculations[14,15] have considered the band folding required to obtain the detailed low-temperature band structure characterizing the CDW phase. The latter calculations are extremely sensitive to small adjustments of the band structure and final determination of the CDW Fermi surfaces will require systematic experimental data on all of the different phases.

In this paper we report new results on the Fermi-surface sections in the CDW phase of $2H$-TaS_2. Both Shubnikov–de Haas oscillations and de Haas–van Alphen oscillations have been used to determine the Fermi-surface cross sections and to examine the dependence of these cross sections on field direction. The results of these measurements are also compared to previous measurements on $4Hb$-TaS_2 and $2H$-$TaSe_2$ crystals in the CDW state. In all of these cases the Fermi-surface sections measured result from a commensurate CDW of wavelength $\lambda_{CDW} = 3a_0$ in the trigonal prismatic layers where a_0 is the lattice vector of the high-temperature phase. The different phases and materials show similar effects of the CDW on the Fermi-surface topology, but distinct differences in detail are observed, and these will be discussed in terms of model calculations.

II. EXPERIMENTAL TECHNIQUES

The ac magnetoresistance, dc resistance, and magnetic susceptibility measurements were made on single crystals of $2H$-TaS_2. The crystals were grown by the method of iodine-vapor transport from stochiometric prereacted powders. $4Hb$-TaS_2 single crystals were grown in a temperature gradient of 720–700 °C for 4–6 weeks. The crystals were then slowly cooled to room temperature over a period of 3 days. This slow cooling procedure allowed the crystals to transform into the $2H$ phase, giving smooth grey polyhedra of relatively high perfection. The top and bottom basal plane facets had mirror surfaces, while the sides showed very fine steps. The crystals were then cleaved or used as grown for use in the susceptibility measurements, and cleaved and cut into bar-shaped specimens for the magnetoresistance and resistivity measurements. Measurements of the residual resistance ratio (RRR) $\rho_{300\ K}/\rho_{4.2\ K}$ were variable ranging from 5 to 200 due to the large temperature-dependent anisotropy, which makes lead placement a critical factor. This was demonstrated by measuring the RRR on a single crystal, cleaving it, and remeasuring the RRR. The RRR varied from 15 to about 60 for one crystal, with 60 being the value for the thinnest section. The strength of the magnetoresistance oscillations seemed to be independent of the measured RRR. Therefore we conclude that the RRR for the current along the layers is greater than 60.

The ac magnetoresistance and dc resistance measurements were carried out with the crystals mounted on a printed circuit block using solder or silver paint contacts. All of the measurements were made with the current parallel to the layers unless otherwise noted. The magnetoresistance and ac susceptibility measurements were made using an ac field modulation technique[16] with second-harmonic detection. For fields up to 70 kG, a

superconducting magnet was used with a second superconducting modulation coil providing a maximum modulation field of about 500 G at 7.5 Hz. The main field was swept through the field range of 10–70 kG. Magnetoresistance measurements were also made in fields up to 150 kG using a Bitter solenoid with field modulation up to 5 kG. The frequencies of the oscillations were analyzed using a fast Fourier transform computer program. The sample was maintained at about 1.1 K in a pumped bath of liquid helium.

The ac susceptibility measurements were made using a compensated pickup coil. The dc susceptibility measurements were made using a Faraday balance technique.[17] A single crystal was suspended in a quartz bucket by a 0.0005-in.-diam tungsten wire with the c axis of the crystal either parallel or perpendicular to the wire. If the c axis is parallel to the wire, the layers of the crystal will be parallel to the field. If the c axis is perpendicular to the wire, the crystal experiences a torque which will align the layers perpendicular to the field. We have determined this by rotating the field direction around the axis of the wire and detecting no change in the susceptibility.

III. EXPERIMENTAL RESULTS

Both resistivity and susceptibility as function of temperature have been measured for the $2H$-TaS_2 single crystals produced by thermal transformation of the $4Hb$-TaS_2 crystals. Data in the temperature range 1–200 K are shown in Figs. 1 and 2.

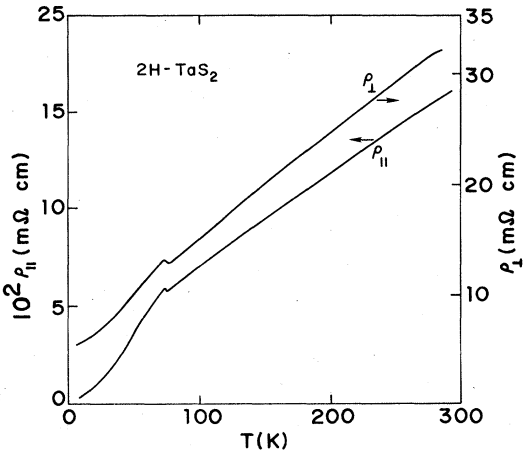

FIG. 1. Resistivity vs temperature for a $2H$-TaS_2 single crystal in the range 4.2–300 K. $\rho_\perp$ and $\rho_{||}$ refer to the resistivity measured for current parallel and perpendicular to the layers. The resistive anomaly at ~ 75 K occurs at the charge-density-wave transition.

In each case the data indicate the existence of a CDW transition at ~75 K as expected for the $2H$ phase. No evidence of CDW transitions resulting from residual $4Hb$-phase regions is observed. The resistivity has been measured for currents both parallel and perpendicular to the layers. The ratio $\rho_\perp/\rho_{||}$ is approximately 200 at room temperature and approximately 2000 at 4.2 K. The ratio at 4.2 K should be considered a minimum, since the parallel resistivity at low temperature is a sensitive function of lead attachment. The measured residual resistance ratios vary from 50 to 80 for current parallel to the layers. Tidman *et*

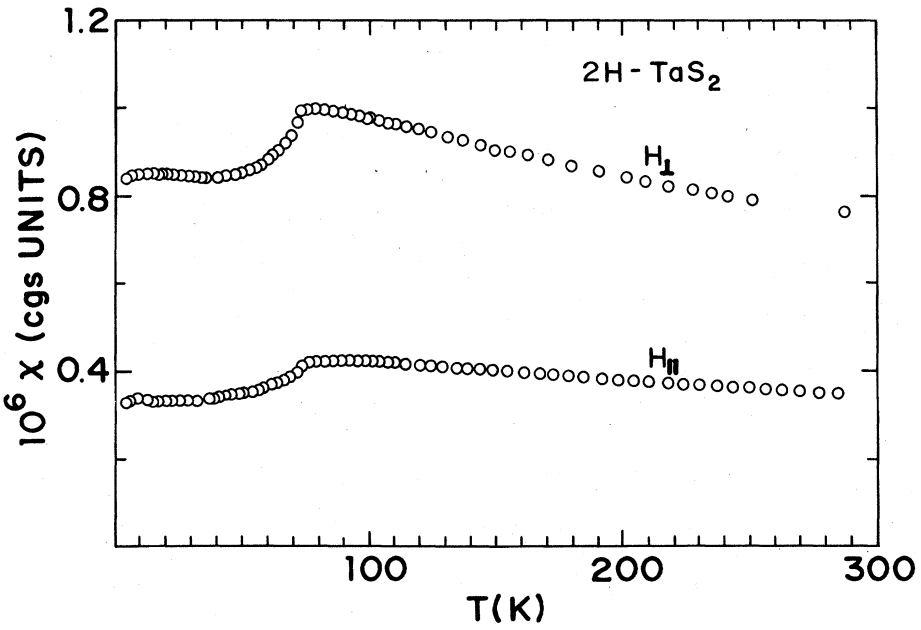

FIG. 2. Magnetic susceptibility vs temperature for a $2H$-TaS_2 single crystal in the range 4.2–300 K. Measurements were made in a magnetic field of 4 kG for field orientations both parallel and perpendicular to the layers. The anomaly at ~ 75 K is characteristic of the charge-density wave.

al.[4] have also measured the resistivity of $2H$-TaS_2 for currents both parallel and perpendicular to the layers, and find a strong rise in $\rho_\perp$ below the CDW transition at 75 K. We do not observe this rise in $\rho_\perp$ and, except for the difference in magnitude, both resistivities show a similar temperature dependence below 75 K, as shown in Fig. 1.

The magnetic susceptibility has been measured with the magnetic field both parallel and perpendicular to the layers, and the ratio $\chi_\perp/\chi_\parallel$ stays within the range 2.2–2.5 over the temperature range 4.2–300 K. The measured values at room temperature were $\chi_\perp = 0.83 \pm 0.3$ emu/g and $\chi_\parallel = 0.36 \pm 0.03$ emu/g. The measured ratio is comparable to the value of 2 measured for $2H$-$TaSe_2$ by Benchimol *et al.*[18]

The above measurements of dc resistivity and susceptibility were made to confirm that the transformed crystals show the CDW transition associated with the pure $2H$ phase, and further analysis of these results will not be included here. The quality of the crystals produced was adequate to observe oscillatory components in both the magnetoresistance and susceptibility, and this paper will concentrate on the measurement of these oscillatory components and their analysis in terms of the Fermi surface in the CDW phase of $2H$-TaS_2.

The Shubnikov–de Haas oscillations have been measured in the range 10–150 kG, while the de Haas-van Alphen (dHvA) oscillations have been measured in the range 10–70 kG. Because of the small size of the crystals, the ac magnetoresistance techniques provide better detection for the weak frequencies. However, both methods give reasonable amplitudes for the strong frequencies, as shown in Figs. 3(a) and 3(b). The Fourier analysis of frequencies obtained from each method is shown in Figs. 4(a) and 4(b) for magnetic field perpendicular to the layers. Good agreement for the three dominant frequencies is obtained, while the lowest frequencies are resolved best in the ac magnetoresistance transforms of data taken at high modulation levels. A Fourier transform emphasizing the lower frequencies is shown in Fig. 5. The frequencies and corresponding cross sections of the Fermi surface for magnetic field perpendicular to the layers are listed in Table I. Eleven frequencies below 2 MG are detected in the magnetoresistance. Five of these are confirmed in the de Haas–van Alphen measurement and a higher frequency of 6.44 MG is detected in the de Haas–van Alphen experiment.

The angular variation of these frequencies has been tracked using ac magnetoresistance, and the results are plotted in Figs. 6(a) and 6(b). The strongest frequencies of 1.35, 0.87, and 0.67 MG follow closely to a $\omega_\perp \sec\theta$ angular dependence as

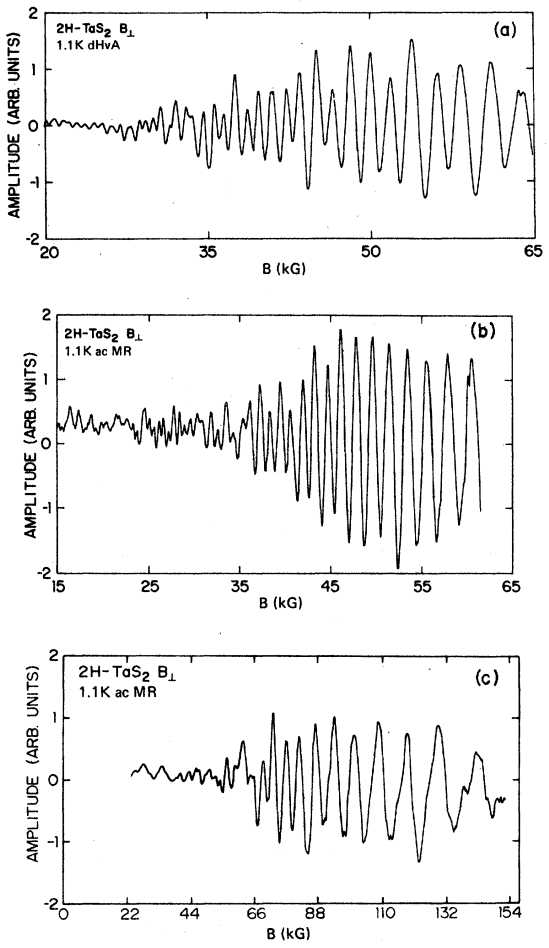

FIG. 3. (a) de Haas–van Alphen oscillations observed in a single crystal of $2H$-TaS_2 in a field range 20–65 kG. (b) Shubnikov–de Haas oscillations observed in a single crystal of $2H$-TaS_2 for the field range 15–60 kG using a field modulation of 500 G peak to peak and harmonic detection. (c) Shubnikov–de Haas oscillations observed in a single crystal of $2H$-TaS_2 for a field range 22–152 kG using a modulation of 5 kG peak to peak and harmonic detection.

represented by the solid lines in Fig. 6(a). The lower frequencies, as shown in Fig. 6(b), deviate from this dependence, and several have minima 20°–30° away from the perpendicular field direction.

It is interesting to compare the above frequencies to results obtained on other layer crystals. Fleming and Coleman[19] reported oscillations in the dc magnetoresistance of $4Hb$-TaS_2 and $2H$-$TaSe_2$, while Graebner[20] has reported de Haas–van Alphen results on $2H$-$TaSe_2$. We have rerun the magnetoresistance measurements on $4Hb$-TaS_2 and $2H$-$TaSe_2$ using ac techniques with improved sensitivity and, aside from small adjustments, confirm the frequencies reported from dc magnetoresistance

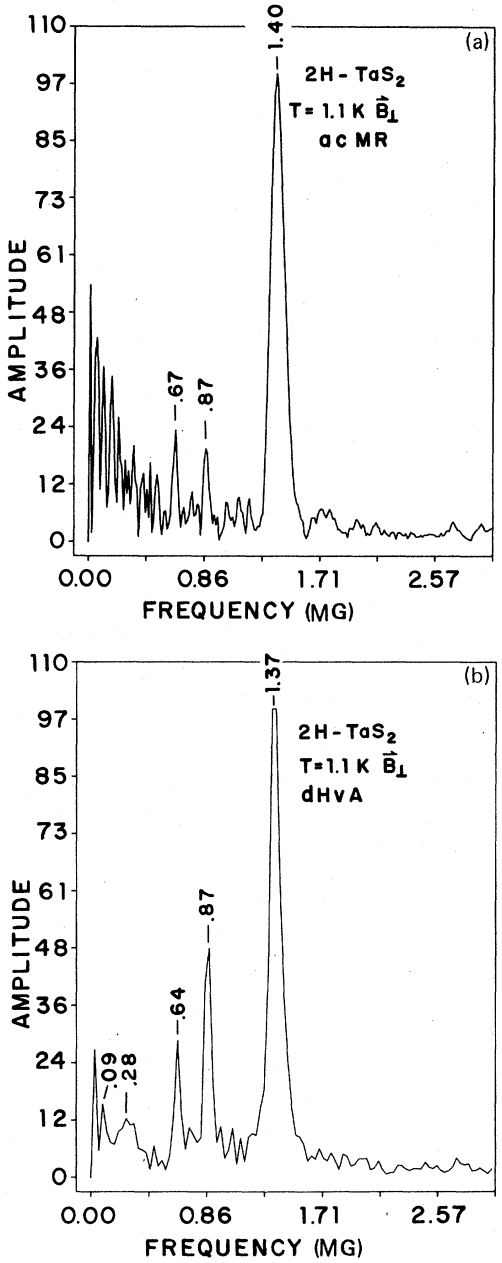

FIG. 4. (a) Fast-Fourier-transform analysis of Shubnikov–de Haas oscillations in Fig. 3(b). (b) Fast-Fourier-transform analysis of de Haas–van Alphen oscillations in Fig. 3(a). Both methods show three dominant frequencies in the range 0.6–1.4 MG.

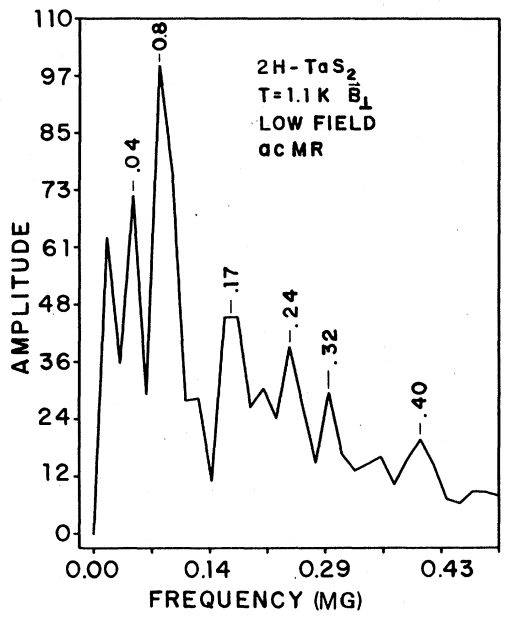

FIG. 5. Fast Fourier transform emphasizing the very-low-frequency oscillations observed in the Shubnikov–de Haas data. These are enhanced by increasing the field-modulation amplitude.

and de Haas–van Alphen results. Table II lists the frequencies measured for $2H$-TaS_2 in the present experiment, along with the frequencies observed for $4Hb$-TaS_2 and $2H$-$TaSe_2$ using ac magnetoresistance.

The low frequencies observed in both $2H$-TaS_2 and $4Hb$-TaS_2 suggest a close correspondence between the number and areas of the Fermi-surface cross sections in these two phases of TaS_2. This is consistent with general theoretical considerations, and further discussion will be given in Sec. IV.

The frequencies in $2H$-$TaSe_2$ are observed to have generally higher values than observed in both phases of TaS_2, and several large orbits are observed that are possibly connected with magnetic breakdown of the CDW gaps. Such large orbits are not observed in either of the TaS_2 phases, but this may be due to lower crystal quality. The very low frequencies in the range 0.04–1.0 MG observed in both phases of TaS_2 are clearly not present in $2H$-$TaSe_2$. In the magnetoresistance of $4Hb$-TaS_2 low frequencies in the range 0.04–1.0 MG in fact contribute the dominant oscillatory amplitudes.

In all of these cases the magnitude and number of the frequencies observed are consistent with the Fermi-surface modifications that are expected to result from the formation of the CDW superlattice. A summary and discussion of the band-structure information and existing model calculations will be given in Sec. IV.

IV. DISCUSSION

The frequencies measured for $2H$-TaS_2 in the present experiment arise from cross sections of Fermi surface that are 50–1000 times smaller than those expected for $2H$-TaS_2 in the high-temperature phase. For the high-temperature Fermi sur-

TABLE I. Shubnikov–de Haas and de Haas–van Alphen frequencies measured for $2H$-TaS_2.

	ac magnetoresistance		dHvA	
	Frequency (MG)	Area (10^{-2} Å^{-2})	Frequency (MG)	Area (10^{-2} Å^{-2})
1			6.44 ± 0.04	6.14 ± 0.04
2	1.80 ± 0.06	1.69 ± 0.06		
3	1.40	1.32	1.37	1.30
4	0.87	0.83	0.87	0.83
5	0.67	0.63	0.64	0.61
6	0.40 ± 0.01	0.38 ± 0.01	•••	•••
7	0.32	0.30	•••	•••
8	0.24	0.23	0.28	0.27
9	0.17	0.16	•••	•••
10	0.08	0.08	0.09	0.09
11	0.04	0.04	•••	•••

face the hole surface at K corresponds to ~50 MG and the hole surface at Γ corresponds to ~40 MG. The appropriate cross sections for $2H$-$TaSe_2$ from the calculations of Wexler and Woolley[11] are shown in Fig. 7. We therefore conclude that the observed Fermi-surface sections are consistent with a CDW superlattice resulting from the formation of triple CDW's in the plane of the layers with $\lambda_{CDW} = 3a_0$. The superlattice zone will have a cross-sectional area perpendicular to the c axis which is equal to $\frac{1}{9}$ of the original zone cross section. The required band folding into this reduced zone can then generate the many small sections observed in the experiment. In this respect, the results on $2H$-TaS_2 follow the same general pattern as observed for $4Hb$-TaS_2 and $2H$-$TaSe_2$, and the model calculations and band folding will be similar.

Band-structure calculations for the high-temperature $2H$ phases of TaS_2 and $TaSe_2$ have been carried out by Wexler and Woolley,[11] by Mattheiss,[12] and by Myron and Freeman.[13] Wilson[15] has constructed a folded version of the Wexler and Woolley band structure for $2H$-$TaSe_2$ in order to analyze frequencies observed in the CDW phase. The CDW produces gapping of the Fermi surface and, by adjustments of the band structure in these regions, Wilson has been able to generate Fermi-surface sections corresponding to the experimental frequencies observed in $2H$-$TaSe_2$. The sections generated by Wilson's folding scheme are

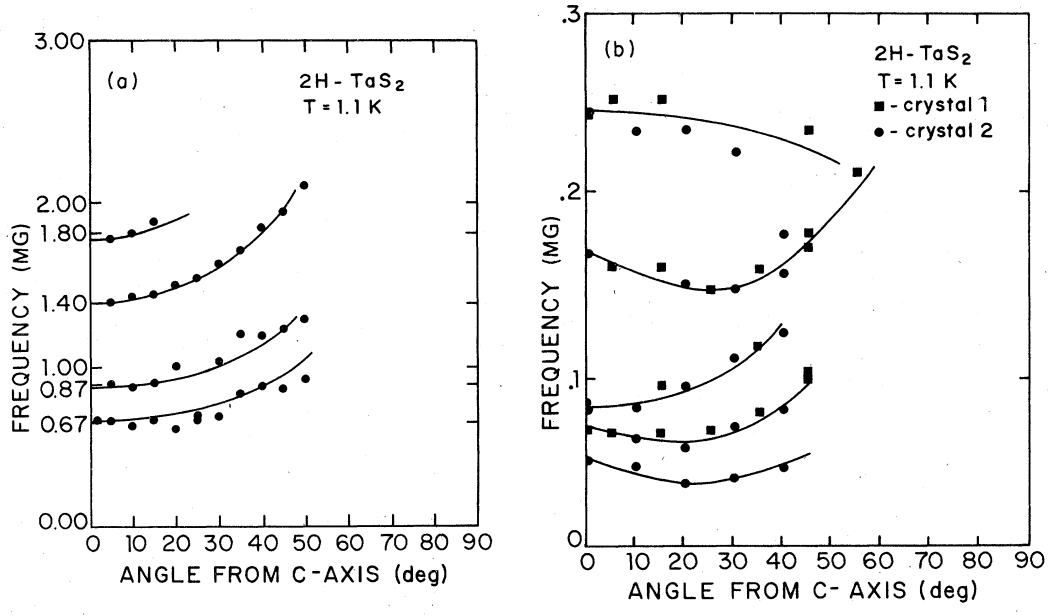

FIG. 6. (a) Angular dependence of the frequencies in the range 0.6–2.0 MG observed in $2H$-TaS_2 for field directions in a range from the c axis to 60° from the c axis. Solid curves represent a plot of $\omega = \omega_\perp \sec\theta$, where $\omega_\perp$ is the frequency for $\vec{H} \| \vec{c}$. (b) Angular dependence of the frequencies below 0.3 MG observed in $2H$-TaS_2. Several of these branches show frequency minima for field directions 20°–30° off the c axis. (θ is measured from the c-axis direction.)

TABLE II. Shubnikov–de Haas frequencies measured for $2H$-TaS_2, $4Hb$-TaS_2, and $2H$-$TaSe_2$.

Frequency (MG)			
$2H$-TaS_2	$4Hb$-TaS_2	$2H$-$TaSe_2$	Theory (RS)
		44.60 ± 0.06 [a]	36.9 [c]
		25.80 [b]	23.9 [c]
		15.80 [b]	
			13.8 [c]
		12.73	
		12.13	
		10.23 [b]	
	8.20 ± 0.06	7.67 [b]	7.2
6.44 ± 0.06			
	4.9	4.84	
	3.6	4.00 [b]	3.63
	3.2	2.62 [b]	
	2.07	2.21 [b]	
	1.90		1.8 [c]
1.80	1.78	1.68 [b]	
	1.56		
1.40	1.30	1.37	
	1.15		
0.87	0.89		0.91
0.67	0.49		0.51
0.40 ± 0.01	0.38 ± 0.01		
0.32	0.35		
0.24	0.27		
0.17	0.15		
0.08			
0.04	0.044 ± 0.005		

[a] Orbits from magnetic breakdown.

[b] Orbits associated with undulating cylinders along the c axis.

[c] From Rice and Scott (RS) calculations including magnetic breakdown (unpublished).

shown in Fig. 8. These sections are drawn representing the average cross sections of the undulating cylinders parallel to the c axis. Each undulating cylinder will contain two extremal areas and will therefore give paired sets of frequency branches as observed[20] for $2H$-$TaSe_2$.

The Shubnikov–de Haas and de Haas–van Alphen frequencies observed in $2H$- and $4Hb$-TaS_2 follow the same general pattern as observed in $2H$-$TaSe_2$. However, the extremely low frequencies observed in both of the TaS_2 phases are not present in $2H$-$TaSe_2$. For field directions parallel to the c axis the low-frequency range in both $2H$- and $4Hb$-TaS_2 is approximately 0.04–1 MG (see Table II), and indicates that for the $4Hb$ phase little change in the trigonal prismatic band structure has occurred due to charge transfer from the $1T$ layers. This is consistent with preliminary theoretical results of Wexler and Woolley,[21] which predict a charge transfer from the octahedral to trigonal prismatic sandwiches of ~2%

The angular variation of the low-frequency

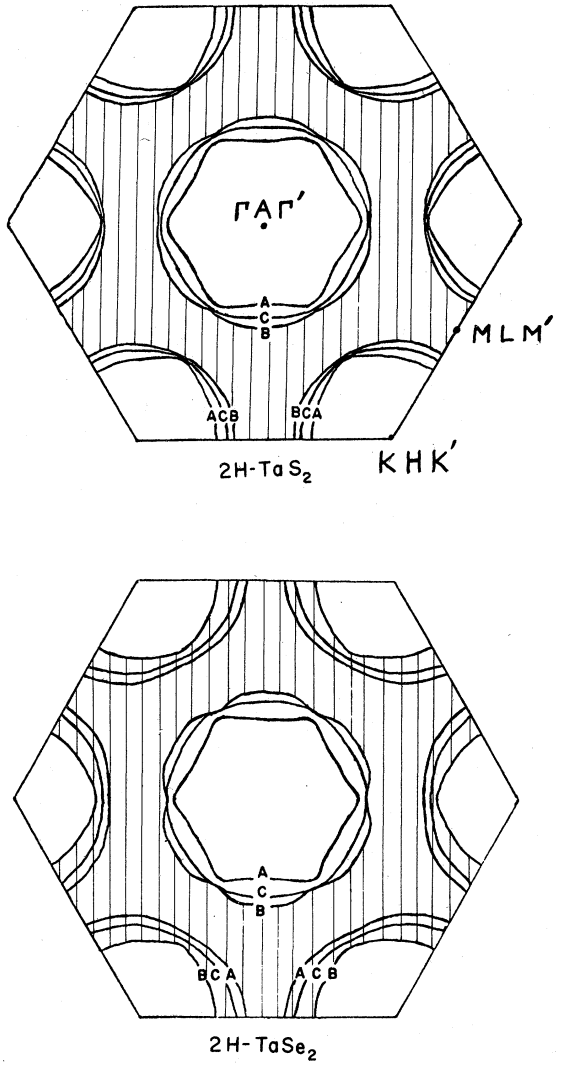

FIG. 7. Cross sections of Fermi surface perpendicular to the c axis for the high-temperature $2H$ phases of TaS_2 and $TaSe_2$ from Wexler and Woolley (Ref. 11). Sections labeled A, B, and C correspond to A, $k_z = 0$; B, $k_z = 2\pi/c$; C, $k_z = \pi/c$. The cross sections indicate a small difference in the size and phase of the undulations in the two materials. The hole surface centered at K (H) corresponds to ~ 50 MG. The hole surface centered at Γ corresponds to ~ 40 MG.

branches in $2H$- and $4Hb$-TaS_2 do, however, show a substantial difference. As measured by dc magnetoresistance and confirmed in the present ac measurements, the low frequencies in $4Hb$-TaS_2 follow almost exactly the $\omega_\perp \sec\theta$ dependence expected for cylinders and shown in Fig. 9. In contrast, as shown in Fig. 6(b), the very low frequencies observed in $2H$-TaS_2 show minima off the c-axis field direction and suggest a substantial c-axis dependence of the energy-band regions contributing to these small sections in the $2H$ phase.

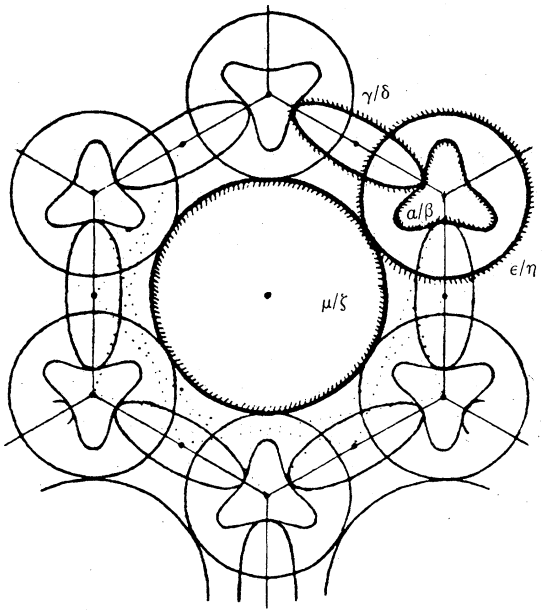

FIG. 8. Fermi-surface cross sections generated for the charge-density-wave phase of $2H$-$TaSe_2$ by Wilson, using a band-folding scheme (Ref. 15). Average cross sections perpendicular to the c axis are shown.

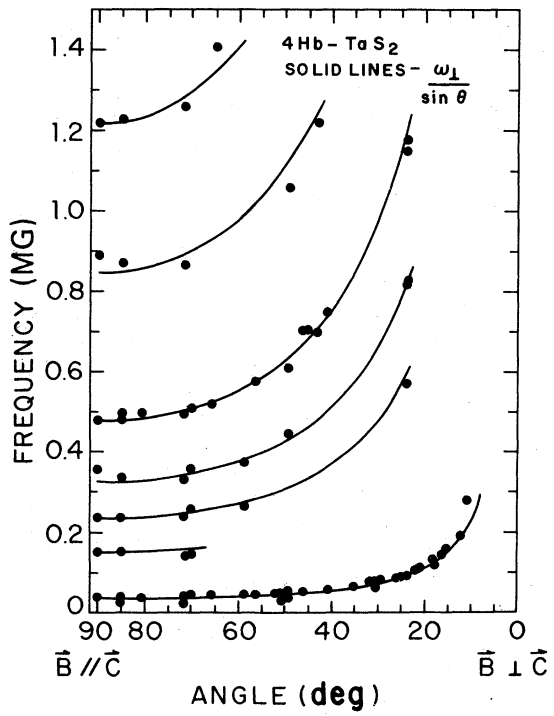

FIG. 9. Angular dependence of the low-frequency oscillations observed in $4Hb$-TaS_2 by Fleming and Coleman (Ref. 20). The solid curves represent plots of $\omega = \omega_\perp / \sin\theta$, where $\omega_\perp$ is the frequency for $\vec{H} \| \vec{c}$. (θ is measured from the plane of the layers.) This is equivalent to $\omega = \omega_\perp \sec\theta$ with θ measured from the c axis.

The more extreme two-dimensional behavior observed in $4Hb$-TaS_2 is, of course, consistent with the extreme conductivity anisotropy and the expected decoupling of the trigonal prismatic layers due to the intervening octahedral layers in the $4Hb$ phase.

Rice and Scott[14] have made a preliminary calculation of the band structure in the CDW phase of TaS_2 using their saddle point mechanism of CDW formation. Using the high-temperature band structure of Mattheiss, and a triple CDW of wavelength $\lambda = 3a_0$, they obtain cross sections corresponding to the frequencies listed in column 4 of Table II. The calculation is strictly two dimensional, and might be expected to apply best to the $4Hb$ phase. Although, as seen in Table II, frequencies down to 0.81 MG are predicted and approximate magnitudes are in agreement with the observed intermediate frequencies, the very low frequencies are not predicted. These very low frefrequencies are connected with fine detail in the band structure, and the above model calculations have not included interactions such as spin-orbit coupling. The initial effect of spin-orbit coupling would, as, for example, in Wilson's model for $2H$-$TaSe_2$ in Fig. 8, open gaps at the crossing points and generate additional frequencies in a range down to 0.6 MG. For TaS_2 a band-folding scheme starting with the high-temperature band structure of $2H$-TaS_2 and following Wilson's procedure might, by suitable adjustment, produce the much lower frequencies. However, the two high-temperature band structures for $2H$-TaS_2 and $2H$-$TaSe_2$ are very similar, as shown in Fig. 7, and whether or not the small differences connected with the difference in undulations along c would generate the additional frequencies in TaS_2 cannot be predicted without carrying out the detailed folding procedure.

The existence of sum and difference frequencies should also be considered. Within the accuracy of the low-frequency measurement, a number of frequency combinations in both $2H$- and $4Hb$-TaS_2 are numerically close enough to be considered. However, the lowest frequency of ~0.04 MG does not fit a sum or difference and in $4Hb$-TaS_2 the lowest frequencies also show the largest amplitudes, which ordinarily would not follow for sum and difference frequencies. Schlottman and Falicov[22] have considered nonlinear effects in CDW systems that could enhance the amplitudes of sum and difference frequencies, but the amplitudes should still be lower by approximately an order of magnitude than those of the two fundamental frequencies involved. Magnetic-breakdown effects might play a role in enhancing the magnetoresistance oscillations, and this possibility needs further investiga-

tion. Previous data on the dc magnetoresistance[19] of $4Hb$-TaS_2 suggested the presence of magnetic breakdown involving the 0.044-MG frequency, and measurements of the Hall effect also confirmed possible magnetic breakdown. A similar behavior in $2H$-TaS_2 has not yet been observed, but further work on the highest quality crystals in higher magnetic fields is required.

V. CONCLUSIONS

Crystal-growing procedures using the iodine-vapor transport method have been used to obtain highly perfect crystals of $2H$-TaS_2, $4Hb$-TaS_2, and $2H$-$TaSe_2$. The $2H$-TaS_2 crystals were obtained by thermally transforming crystals initially grown in the $4Hb$ phase. Oscillatory components of the magnetoresistance have been measured using ac field modulation and harmonic detection. de Haas-van Alphen oscillations have also been detected and confirm the frequencies measured by magnetoresistance, although the magnetoresistance measurements are more sensitive for the smaller specimens and lowest frequencies.

All of the results reflect the existence of Fermi-surface sections which result from the charge-density-wave gapping and the required band folding of the high-temperature band structure. In comparing $2H$-TaS_2 and $2H$-$TaSe_2$, the major difference in Fermi surface appears to be the existence of approximately ten frequencies in $2H$-TaS_2 below 1 MG, while $2H$-$TaSe_2$ shows no frequencies below 1.37 MG. Both materials show frequencies in the range 1–10 MG, while $2H$-$TaSe_2$ shows frequencies well above 10 MG, some of which may result from magnetic breakdown.

Comparison of the observed frequencies in the $2H$ and $4Hb$ phases of TaS_2 shows that approximately the same range and number of frequencies are observed, indicating that charge transfer from the octahedral to trigonal prismatic layers in the $4Hb$ phase is relatively small. Comparison of the angular dependence of the frequencies in $2H$- and $4Hb$-TaS_2 shows that the small sections in the $4Hb$ phase are much more two dimensional than in the $2H$ phase. All of the data are generally consistent with model calculations and band-folding procedures, although the extremely low frequencies are not predicted by present models. The present experiments provide the numerical values for Fermi-surface cross sections, and these can be used as a guide to refinement of the model calculations. The differences in Fermi-surface topologies for the charge-density-wave states in two phases of TaS_2 have been established experimentally and can also be used to develop the subtle differences between the CDW phases of TaS_2 and $TaSe_2$ necessary for accurate model calculations.

Additional work on the temperature dependence of amplitudes and more extended work at high magnetic fields should provide information on effective masses and possible magnetic-breakdown effects.

ACKNOWLEDGMENTS

The authors would like to thank Estelle S. Phillips, John A. Polo, Jr., and Dr. Robert M. Fleming for their assistance. We would also like to thank Dr. J. A. Wilson, Professor V. Celli, and Professor L. M. Falicov for many useful discussions. We are grateful to Professor A. M. Wexler for sending us his unpublished calculations on $4Hb$-TaS_2. This work was supported by the U. S. Department of Energy Contract No. EY-76-5-05-3105. Work above 80 KG was performed while the authors were guest scientists at the Francis Bitter National Magnet Laboratory, which is supported at MIT by the NSF.

[1]J. A. Wilson and A. D. Yoffe, Adv. Phys. 18, 1932 (1969).
[2]H. N. S. Lee, M. Garcia, H. McKinzie, and A. Wold, J. Solid State Chem. 1, 190 (1970).
[3]J. A. Wilson, F. J. DiSalvo, and S. Mahajon, Adv. Phys. 24, 117 (1975).
[4]J. P. Tidman, O. Singh, A. E. Curzon, and R. F. Frindt, Philos. Mag. 30, 1191 (1974).
[5]R. A. Craven and S. F. Meyer, Phys. Rev. B 16, 4583 (1977).
[6]F. J. DiSalvo, B. G. Bagley, J. M. VoorHoeve, and J. V. Waszcak, J. Phys. Chem. Solids 34, 1357 (1973).
[7]P. M. Williams, G. S. Parry, and C. B. Scruby, Philos. Mag. 29, 695 (1974).
[8]D. E. Moncton, J. D. Axe, and F. J. DiSalvo, Phys. Rev. Lett. 35, 120 (1975).
[9]F. J. DiSalvo, D. E. Moncton, J. A. Wilson, and S. Mahajon, Phys. Rev. B 14, 1543 (1976).
[10]D. E. Moncton, F. J. DiSalvo, J. D. Axe, L. J. Sham, and B. R. Patton, Phys. Rev. B 14, 3432 (1976).
[11]G. Wexler and A. M. Woolley, J. Phys. C 9, 1185 (1976).
[12]L. F. Mattheiss, Phys. Rev. B 8, 3719 (1973).
[13]H. W. Myron and A. J. Freeman, Phys. Rev. B 11, 2735 (1975).
[14]T. M. Rice and G. K. Scott, Phys. Rev. Lett. 35, 120 (1975).
[15]J. A. Wilson, Phys. Rev. B 15, 5748 (1977).
[16]J. R. Anderson and D. R. Stone, in *Experimental Physics*, edited by R. V. Coleman (Academic, New York, 1974), p. 33.
[17]B. L. Morris and A. Wold, Rev. Sci. Instrum. 39, 1937 (1968).
[18]J. B. Benchimol, F. T. Hedgcock, and F. J. DiSalvo

(unpublished).
[19]R. M. Fleming and R. V. Coleman, Phys. Rev. B 16, 302 (1977).
[20]J. E. Graebner, Solid State Commun. 21, 353 (1977).
[21]G. Wexler and A. M. Woolley (unpublished).
[22]P. Schlottman and L. M. Falicov, Phys. Rev. Lett. 38, 855 (1977).